Accepted Manuscript

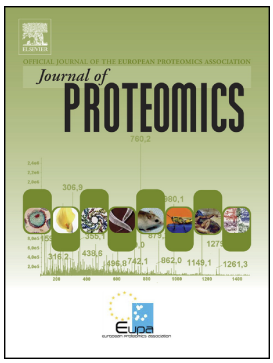

Integrative transcriptome and proteome analyses define marked differences between Neospora caninum isolates throughout the tachyzoite lytic cycle

P. Horcajo, D. Xia, N. Randle, E. Collantes-Fernández, J. Wastling, L.M. Ortega-Mora, J. Regidor-Cerrillo

PII: S1874-3919(17)30378-0
DOI: doi:10.1016/j.jprot.2017.11.007
Reference: JPROT 2969

To appear in: *Journal of Proteomics*

Received date: 9 August 2017
Revised date: 25 October 2017
Accepted date: 9 November 2017

Please cite this article as: P. Horcajo, D. Xia, N. Randle, E. Collantes-Fernández, J. Wastling, L.M. Ortega-Mora, J. Regidor-Cerrillo , Integrative transcriptome and proteome analyses define marked differences between Neospora caninum isolates throughout the tachyzoite lytic cycle. The address for the corresponding author was captured as affiliation for all authors. Please check if appropriate. Jprot(2017), doi:10.1016/j.jprot.2017.11.007

Integrative transcriptome and proteome analyses define marked differences between *Neospora caninum* isolates throughout the tachyzoite lytic cycle

P. Horcajo[1¥], D. Xia[2¥], N. Randle[3], E. Collantes-Fernández[1], J. Wastling[4], L.M. Ortega-Mora[1], J. Regidor-Cerrillo[1*].

[1] SALUVET, Animal Health Department, Faculty of Veterinary Sciences, Complutense University of Madrid, Ciudad Universitaria s/n, 28040 Madrid, Spain.

[2] The Royal Veterinary College, Royal College Street, London, NW1 0TU, United Kingdom.

[3] Department of Infection Biology, Institute of Infection & Global Health, University of Liverpool, Liverpool Science Park IC2, 146 Brownlow Hill, Liverpool, L3 5RF, United Kingdom.

[4] Faculty of Natural Sciences, Keele University, Keele, Staffordshire, ST5 5BG, United Kingdom.

[¥]Authors contributed equally

*Corresponding author: Javier Regidor Cerrillo, Animal Health Department, Faculty of Veterinary Sciences, Complutense University of Madrid, Ciudad Universitaria s/n 28040, Madrid, Spain. E-mail: jregidor@ucm.es

Co-authors e-mail addresses: PH: phorcajo@ucm.es; DX: dxia@rvc.ac.uk; NR: Nadine.Randle@liverpool.ac.uk; ECF: esthercf@ucm.es; JW: j.wastling@keele.ac.uk; LMOM: luis.ortega@ucm.es; JRC: jregidor@ucm.es

Abstract

Neospora caninum is one of the main causes of transmissible abortion in cattle. Intraspecific variations in virulence have been widely shown among *N. caninum* isolates. However, the molecular basis governing such variability have not been elucidated to date. In this study label free LC-MS/MS was used to investigate proteome differences between the high virulence isolate Nc-Spain7 and the low virulence isolate Nc-Spain1H throughout the tachyzoite lytic cycle. The results showed greater differences in the abundance of proteins at invasion and egress with 77 and 62 proteins, respectively. During parasite replication, only 19 proteins were differentially abundant between isolates. The microneme protein repertoire involved in parasite invasion and egress was more abundant in the Nc-Spain1H isolate, which displays a lower invasion rate. Rhoptry and dense granule proteins, proteins related to metabolism and stress responses also showed differential abundances between isolates. Comparative RNA-seq analyses during tachyzoite egress were also performed, revealing an expression profile of genes associated with the bradyzoite stage in the low virulence Nc-Spain1H isolate. The differences in proteome and RNA expression profiles between these two isolates reveal interesting insights into likely mechanisms involved in specific phenotypic traits and virulence in *N. caninum*.

Keywords: *Neospora caninum*, low and high virulence isolates, proteome, transcriptome

1. Introduction

Neospora caninum is a cyst-forming obligate intracellular protozoan parasite that is closely related to *Toxoplasma gondii*, which infects different domestic or wild canids as its definitive host and cattle and other ungulates as intermediate hosts [1]. *N. caninum* has been recognized as one of the main causes of abortion in cattle, resulting in devastating economic losses to the beef and dairy industries [2]. Although various factors are potentially involved in determining the dynamics of *N. caninum* infection, experiments in pregnant cattle have shown the key role of different isolates of *N. caninum* in the severity of disease and its capacity to cause foetal mortality in cattle [3-6]. Host tissue damage occurs as a consequence of the tachyzoite lytic cycle, a process that enables parasite propagation and involves the following successive steps: parasite invasion, adaptation to new intra-cytoplasmatic conditions, intracellular proliferation and egress from host cells [7,8]. Interestingly, the *in vitro* behaviour of a *N. caninum* population in these processes has demonstrated the potential association of the phenotypic traits such as the invasion rate and tachyzoite yield with pathogenicity observed in animal models [9-11]. Nevertheless, the molecular basis and mechanisms that govern such biological diversity in *N. caninum* remain largely unknown. *N. caninum* appears to be highly conserved genetically [12], although previous proteomic approaches have identified some differences between isolates [13-15]. Differences in secretory elements (rhoptry and dense granule proteins) and protein related to gliding motility and oxidative stress have been described among *N. caninum* isolates showing variations in protein expression, post-translational modifications and protein turnover [15]. Recently, an *in vitro* study comparing host cell modulation by *N. caninum* isolates with high (Nc-Spain7) and low (Nc-Spain1H) virulence has shown a great similarity in host transcriptome modulation by both isolates but marked differences in the parasite

transcriptome between isolates [16]. In this study, we used a global approach to examine the changes between the *N. caninum* Nc-Spain7 and Nc-Spain1H isolates throughout the fast replicating tachyzoite lytic cycle. We exploited label free LC-MS/MS technology to investigate in deep proteome differences across the tachyzoite lytic cycle: after tachyzoite invasion and adaptation in the host cell at 12 hours post infection (hpi), during active parasite replication at 36 hpi and at early egress at 56 hpi. Furthermore, we analysed the transcriptome status of Nc-Spain7 and Nc-Spain1H using RNA-seq during tachyzoite egress from the host cell. We determined specific patterns of protein abundance for each isolate in each phase of the lytic cycle studied and differences between gene expression profiles that reveal interesting insights into differences in virulence between these two isolates.

2. Materials and methods

2.1 Parasite culture

Parasites were cultured in confluent Marc-145 cultures as previously described [17]. Briefly, medium from Marc-145 cultures grown for 24 h in DMEM with 10% of heat inactivated FBS and 1% antibiotic-antimycotic solution (Gibco, Gaithersburg, MD, USA) was replaced with DMEM supplemented with 2% FCS and 1% of antibiotic-antimycotic solution. Then, cell monolayers were inoculated with an adjusted multiplicity of infection (MOI) of Nc-Spain1H and Nc-Spain7 tachyzoites for parasite passaging onto a new Marc-145 monolayer each three – four days. All experiments in this study were conducted with tachyzoites from both isolates with a limited number of passages (Nc-Spain1H and Nc-Spain7, passage 13-18). All inoculations in *in vitro* assays were performed within one hour after tachyzoite collection from flasks.

2.2 Experimental design and tachyzoite production for proteome and transcriptome analyses

The overall experimental design is shown in Fig. 1. All experiments were carried out with three biological replicates.

Confluent 24-h Marc-145 DMEM free of phenol red (Gibco, Gaithersburg, MD, USA) and FBS were inoculated with purified Nc-Spain1H tachyzoites at a MOI of 7 and Nc-Spain7 tachyzoites at a MOI of 4. Cell monolayers were recovered at 12 hpi (after completion of invasion and prior to tachyzoite duplication), at 36 hpi (active proliferation in the parasitophorous vacuole) and at 56 hpi (early egress), from T75 cm^2 flasks by cell scraping in 5 ml of PBS supplemented with protease and phosphatase inhibitor cocktail (Sigma-Aldrich, St. Louis, MO, USA), passaged by 25 G needles for host cell disruption and purified using PD-10 (Sephadex G-25 columns -GE-Healthcare, Barrington, IL, USA). Tachyzoite purification was carried out at 4ºC. The number and viability of tachyzoites was determined by trypan blue exclusion followed by counting in a Neubauer chamber. Tachyzoites were pelleted by centrifugation at 1,350 x g for 10 min. and stored at – 80ºC until tachyzoite proteome (TZP) analysis.

Tachyzoite samples for transcriptome analysis were obtained as described above. Cell cultures were recovered at 56 hpi, and tachyzoites were purified using PD10 columns as described above. Tachyzoite pellets were directly resuspended in 300 µl of RNAlater (Invitrogen, Carlsbad, CA, USA) and stored at – 80ºC until RNA extraction.

The tachyzoite growth and lytic cycle was monitored daily by microscopy, and photomicrographs for each time-point of sample collection were obtained at 400x on an inverted microscope (Nikon Eclipse E400) connected to a digital camera for checking lytic cycle progression and sample collection in the programmed lytic cycle phases (Fig.1A).

2.3 LC-MS/MS analyses

Detailed materials and methods for sample preparation, LC-MS/MS, proteome data analysis, and Western blot validation are shown in Supplementary file 1. Briefly, prior to trypsin digestion, tachyzoite pellets were resuspended in 25 mM ammonium bicarbonate and RapiGest^{TM} (Waters MS Technologies, Milford, MA, USA) for protein solubilization, reduced with DTT and alkylated with iodocetamide for trypsin digestion. Then, the digests were analysed using an LC-MS/MS system comprising an Ultimate 3000 nano system coupled to a Q-Exactive mass spectrometer (Thermo Fisher Scientific, Waltham, MA, USA). Reversed-phase liquid chromatography was performed using the Ultimate 3000 nanosystem by a linear gradient of 5-40% solvent B (80% acetonitrile in 0.1% formic acid) in 0.1% formic acid (solvent A). The Q-Exactive was operated in data-dependent mode with survey scans acquired at a resolution of 70,000 at m/z 200. Up to the top 10 most abundant isotope patterns were selected and fragmented by higher energy collisional dissociation with normalized collision energies of 30. The maximum ion injection times for the survey scan and the MS/MS scans were 250 and 100 ms, respectively.

For proteome data analyses, the Thermo RAW files were imported into Progenesis QI (version 2.0, Nonlinear Dynamics, Durham, CA, USA). Replicate runs were time-aligned using default settings and an auto-selected run as a reference. Spectral data were transformed into .mgf files with Progenesis QI and exported for peptide identification using the Mascot (version 2.3, Matrix Science, London, UK) search engine and the database ToxoDB-26_N*caninum* LIV_Annotated Proteins (version 26, ToxoDB). The false discovery rates were set at 1% and at least two unique peptides were required for reporting protein identifications. Finally, protein abundance (iBAQ) was calculated as

the sum of all the peak intensities (from the Progenesis output) divided by the number of theoretically observable tryptic peptides for a given protein (Fig. 1B).

The mass spectrometry proteomics data have been deposited in the ProteomeXchange Consortium via the PRIDE [18] partner repository with the dataset identifier PXD007062.

The identified proteins were classified according to their parasite localization and functionality according to the Gene Ontology (GO) terms (annotated and predicted) on the ToxoDB website [19] for the Nc-Liverpool isolate (ToxoDB-26_N*caninum*LIV_AnnotatedProteins), *T. gondii* syntenic homologues (version 26, ToxoDB) and previous reports [20-22].

Validation of LC-MS/MS results was performed by measuring the differential abundance of the proteins MIC2 (NCLIV_022970), ROP2 (NCLIV_001970), and NTPase (NCLIV_068400) between isolates by Western blot analyses using the SAG1 protein (NCLIV_033230) as a housekeeping gene as previously described [23,24]. Images from WB membranes were obtained using a GS-800 Scanner (Bio-Rad Laboratories, Hercules, CA, USA) and were analysed with Quantity One quantification software v. 4.0 (Bio-Rad Laboratories, Hercules, CA, USA) for protein quantification.

2.4 RNA extraction, sequencing and detection of differential mRNA expression

Total RNA was isolated from purified tachyzoites using an RNeasy Mini kit (Qiagen, Hilden, Germany). RNA-Seq was undertaken at the Centre for Genomic Research, University of Liverpool. Briefly, polyadenylated RNA was purified using the Dynabeads® mRNA purification kit (Invitrogen, Carlsbad, CA, USA) and used to prepare RNA-Seq libraries with the Epicentre ScriptSeq v2 RNA-Seq Library Preparation kit (Illumina, San Diego, CA, USA). Libraries were sequenced on the HiSeq2500 (Illumina, San Diego, CA, USA) as 2 x 100-bp paired-end sequencing using

rapid-run mode chemistry. Filtered sequencing reads were aligned against the reference genome of *N. caninum* (NcLiv26; ToxoDB.org) by the TopHat2 aligner and processed with the Cufflinks software (version 2.1.1) to assemble transcripts, quantify expression levels and analyse differentially expressed genes (DEGs) (Fig. 1C).

Validation of transcript expression was performed on three additional biological replicates of tachyzoite samples at 56 hpi prepared as described above using SYBR green quantitative PCR. More detailed material and methods for RNAseq and validation by quantitative real-time PCR are provided in Supplementary file 1.

2.5 *In vitro* invasion analysis

The invasion capacity of *N. caninum* isolates was determined in a plaque assay in which 100 purified tachyzoites of each isolate per well were added to MARC-145 monolayers in 24-well culture plates as previously described [10]. Briefly, the plates were incubated at 37ºC in a 5% CO2-humidified incubator for 48 h, and cell monolayers were labelled by immunofluorescence using anti-tachyzoite hyperimmune rabbit antiserum (1:4000) as the primary antibody and Alexa 594-conjugated goat anti-rabbit secondary antibody (1:1000) (Molecular Probes, Eugene, Oregon, USA). Plate wells were examined using a fluorescence-inverted microscope Nikon Eclipse E400 (Nikon Instruments Europe) at a magnification of 200x to count the labelled parasitophorous vacuoles and lysis plaques (events) per well after parasite growth. Differences between isolates in invasion rates were determined using the U Mann-Whitney test.

2.6 Tachyzoite cell cycle analysis

The cell cycle phase of the tachyzoite culture was studied by flow cytometry. Tachyzoite samples were obtained under the same conditions as detailed previously for proteomic and transcriptome analyses. Purified tachyzoites were pelleted for 10 min at 1350×g and resuspended in 70% (v/v) ethanol with constant shaking, pelleted and

resuspended in PBS. Fixed tachyzoites were labelled by indirect immunofluorescence (IFI) for the differentiation of individual parasites from those forming aggregates. Tachyzoites were permeabilised with PBS containing 3% BSA and 0.25% Triton X-100 for 30 min at 37ºC and labelled using anti-tachyzoite mouse antiserum (1:50 dilution) as the primary antibody and a FITC-conjugated goat anti-mouse IgG at 1:1,000 dilution (Molecular Probes, Eugene, Oregon, USA) as the secondary antibody. Then, the parasites were treated with 250 U RNase A (Ambion, Austin, TX, USA) in the dark for 30 min, resuspended in BD CellFIX™ (Becton-Dickinson, Erembodegem, Belgium), and stained with propidium iodide (PI) (1 μg/ml final concentration). Tachyzoite populations with lower FITC fluorescence were separated as individual tachyzoites. The nuclear DNA content was measured based on the PI fluorescence using a 488 nm argon laser and a Becton-Dickinson FACSCalibur flow cytometer (Becton-Dickinson, Erembodegem, Belgium). Fluorescence was collected in linear mode (10 000 events), and the results were quantified using CELLQuest™ v3.0 (Becton-Dickinson, Erembodegem, Belgium). The percentages of G1 (1 N), S (1–2 N) and G2+M (2 N) tachyzoites were calculated based on defined gates for each population. Two biological replicates were analysed for each isolate.

3. Results and discussion

3.1 Nc-Spain1H and Nc-Spain7 tachyzoite proteomes resemble fast-growing, metabolically active and invasive tachyzoites

A total of 1,390 proteins were identified with high confidence (FDR< 1% and containing at least two uniquely identified peptides) and quantified using Progenesis software for the Nc-Spain1H and Nc-Spain7 isolates across the tachyzoite lytic cycle. The identified proteins covered ~19.6% of the predicted *N. caninum* proteins deposited

in the UniProt database (7,111 predicted proteins, UniProtKB; UP000007494, *Neospora caninum* strain Liverpool) [25]. Raw data are deposited in ProteomeXchange under identifier PXD007062. Each individual identified and quantified protein was categorized by the cellular component and functional prediction. Of the proteins, 14.5% had an unknown localization. Proteins with cytoplasmic (18.49%), nuclear (16.26%) and mitochondrial (11.15%) localizations were also highly represented, followed by proteins associated with the plasma membrane (glycolipid-anchored SAG1-related sequences [SRS] and other proteins localized in the plasma membrane) (9.78%). Proteins from secretory organelles (including micronemes, rhoptries and dense granules) represented approximately 5% (corresponding to 70 proteins) of all those identified proteins (Supplementary Fig. 1A and supplementary file 2). A total of 66.47% of 1,390 proteins from the TZP were assigned to a functional category (Supplementary Fig. 1B and supplementary file 2). The most represented functional categories included proteins involved in metabolism (12%), cellular transport (10%), protein synthesis (9.57%) and protein fate (9.35%). As expected, protein localization and functional profiles identified in both *N. caninum* isolates corresponded to the proteome for the fast growing, metabolically active and invasive tachyzoites.

3.2 Relative quantification demonstrated different proteomes for Nc-Spain1H and Nc-Spain7 throughout the tachyzoite lytic cycle

Progenesis analysis detected 351 proteins at 12 hpi, 136 proteins at 36 hpi and 214 proteins at 56 hpi, with a significant increase or decrease in relative abundance between Nc-Spain1H and Nc-Spain7 TZPs ($q < 0.05$) (Supplementary file 3). These results demonstrated marked differences in the TZP throughout the lytic cycle between the Nc-Spain1H and Nc-Spain7 isolates. Focusing on significant changes ($q < 0.05$) in the relative abundance with a fold change ≥ 2 between the Nc-Spain1H and Nc-Spain7

isolates, there were 77, 19 and 62 proteins with differing abundance at 12 , 36 and 56 hpi, respectively (Fig. 2A, B and C, respectively and Supplementary file 3). Most of the proteins that were differentially abundant between isolates were unique to each time-point of the tachyzoite lytic cycle (Fig. 3 and supplementary file 4). There were only 7 out of 82 Nc-Spain1H proteins and 2 out of 36 Nc-Spain7 proteins that were consistently more abundant across the tachyzoite lytic cycle.

Enriched GO terms or pathways associated with a particular isolate were not found likely due to the high proportion of hypothetical proteins. Nonetheless, differences in the abundance of proteins belonging well-established categories related with invasion machinery, metabolism and response to stress were found between isolates and are detailed below (Fig. 4).

The proteome results from LC-MS/MS were confirmed by WB analyses with available antibodies. The WB results provided similar results to the LC-MS/MS quantification with a higher abundance of NcMIC2 at 12 and 56 hpi in the Nc-Spain1H isolate and a similar protein abundance of NcROP2 and NcNTPase in both isolates (Supplementary Fig. 2).

3.3 Abundance of proteins involved in host cell attachment and invasion varied between Nc-Spain1H and Nc-Spain7 tachyzoite proteomes

Surface antigens differ in abundance between Nc-Spain1H and Nc-Spain7 tachyzoite proteomes.

Members of the SRS protein family were differentially abundant between the Nc-Spain1H and Nc-Spain7 isolates. SRS antigens exert a relevant role in host cell attachment, modulation and evasion of host immunity, and the regulation of virulence [26-28]. An orthologue of, but not syntenic to, TgSAG3 (NCLIV_034740) throughout the tachyzoite lytic cycle and an orthologue of SRS67 (NCLIV_046140) at 56 hpi were significantly more abundant in Nc-Spain1H. More interestingly, NcSAG4

(NCLIV_019580) showed larger fold changes at all time-points in Nc-Spain1H, with the greatest differences compared with Nc-Spain7 at 36 and 56 hpi (12.8-fold and 14.6-fold, respectively). NcSAG4 has been described as a *N. caninum* bradyzoite stage-specific marker [29]. Furthermore, SRS6 (NCLIV_010050), which has been found over-expressed in bradyzoites of *T. gondii* [30], was also significantly more abundant in Nc-Spain1H at 56 hpi. Bradyzoite development of *T. gondii* has been correlated with a reduction in the tachyzoite growth rate [31]. Nc-Spain1H has shown a low *in vitro* growth rate [9] which may facilitate the conversion to the bradyzoite, although has been previously shown that Nc-Spain1H produce only intermediate bradyzoites *in vitro* [32]. The transcriptome analysis, which is detailed in the next section, could corroborate the hypothesis of a pre-bradyzoite stage in Nc-Spain1H since an important bradyzoite gene profile was found to be over-expressed in this isolate. The only SRS protein that was more abundant in Nc-Spain7 throughout the lytic cycle was the orthologue of SRS39 (NCLIV_023620), which is also predominantly expressed during the bradyzoite stage of in the *T. gondii* [30]. It could be interesting to determine the relevance of SRS39 in *N. caninum*.

The microneme protein repertoire is more abundant in Nc-Spain1H tachyzoites, but Nc-Spain1H displays a lower invasion rate.

Micronemes in Apicomplexan parasites are specialized secretory organelles that are critical for essential cellular processes such as attachment and penetration [33]. A total of 9 microneme (MIC) proteins were significantly more abundant in Nc-Spain1H at 56 hpi, and most of them were also more abundant in Nc-Spain1H at 12 hpi, four with FC > 2 and the other four with FC very close to 2 (> 1.8). Only MIC8 (NCLIV_062770) had a higher abundance at 12 hpi but not at 56 hpi. At 36 hpi, differences in the abundance of MIC proteins were not found. Among MIC proteins with higher

abundance in Nc-Sapin1H, orthologues assembling the main TgMIC complexes (MIC1 [NCLIV_043270]/MIC4 [NCLIV_002940] /MIC6; MIC2 [NCLIV_022970]/M2AP [NCLIV_051970]; and MIC8 [NCLIV_062770]/MIC3 [NCLIV_010600]) and others as MIC2-like1 (NCLIV_033690), MIC10 (NCLIV_066250), MIC11 (NCLIV_020720) and MIC17B (NCLIV_038110) were identified. Some of these proteins have been characterized in *N. caninum* and have been associated with invasion processes [34-37]. In contrast to these results, in previous work comparing changes in the proteome expression between these two isolates using DIGE, NcMIC1 was found more abundant in the highly virulent isolate Nc-Spain7 [15]. However, these contrasting results are likely due to differences in techniques, considering that DIGE analysis detects variations in protein species that are likely also attributed to post-translational modifications. NcAMA1 (NCLIV_028680), which is also involved in *N. caninum* invasion [38], was also increased in Nc-Spain1H TZP at 12 and 56 hpi.

In addition to MIC proteins, proteases involved in micronemal protein processing or that contribute to microneme-dependent processes, such as egress, gliding motility, and parasite invasion of host cells, were also more abundant in Nc-Spain1H. Orthologues of the protease SUB1 (NCLIV_021050), which is involved in micronemal protein processing [39], the metalloproteinase toxolysin 4, TLN4, (NCLIV_044230) and the cathepsin L-like protease CPL (NCLIV_004380), proteinase localized outside the micronemes in the vacuolar component, which in *T. gondii* contributes to the proteolytic maturation of proTgM2AP and proTgMIC3 [40], were also found more abundant in Nc-Spain1H at 12 hpi (SUB1) and at 56 hpi (SUB1, TLN4 and CPL). Similarly, PLP1 (NCLIV_020990), a perforin-like protein secreted from micronemes that likely plays a role in parasite egress more than invasion [41], and an orthologue of the chitinase-like protein CLP1 (NCLIV_000740) related to macrophage stimulation to release pro-

inflammatory cytokines in *T. gondii* [42], were more abundant in Nc-Spain1H at 12 (PLP1) and at 56 hpi (PLP1 and CLP1).

All these results seem to indicate that the low virulent isolate Nc-Spain1H has powerful machinery involved in host cell attachment and invasion. In this study, we tested the ability of Nc-Spain1H and Nc-Spain7 to invade host cells. The Nc-Spain1H showed a significant reduction of host invasion ($p < 0.005$) in comparison to Nc-Spain7 (Fig. 5A), as demonstrated in previous work [9,11]. Considering these results, the Nc-Spain1H isolate may be compromised in other unknown mechanisms that are relevant for attachment/invasion processes and the over-expression of all of these factors could be an attempt to compensate for some other deficiency.

Rhoptry proteins also differ in abundance between isolates.

Rhoptry proteins are recognized as one of the major virulence factors in *T. gondii* [43,44]. Three proteins from rhoptries had different abundances between isolates. NcROP1 (NCLIV_069110), which is involved in early invasion [45], showed an approximately 2-fold higher abundance in Nc-Spain1H at 12 and 56 hpi. Interestingly, a predicted member of the rhoptry kinase family ROP20 specific for *N. caninum* (NCLIV_068850), which is orthologous, but not syntenic, to the *T. gondii* virulence factor ROP24 had greater abundance in the highly virulent isolate Nc-Spain7 across the lytic cycle. The orthologue of the bradyzoite pseudokinase 1, BPK1 (NCLIV_007770) was also more abundant in the Nc-Spain7 isolate across the lytic cycle. BPK1 plays a crucial role in the *in vivo* development of *Toxoplasma* cysts [46]. The abundances of BPK1 and SRS39 in Nc-Spain7 are inconsistent with those other bradyzoite-related proteins that were more abundant in the Nc-Spain1H. It remains to be determined if there is a functional role for these proteins in the tachyzoite stage of *N. caninum*.

3.4 Metabolic processes are differentially regulated between Nc-Spain1H and Nc-Spain7 isolates

Gluconeogenesis is up-regulated in the low virulent isolate Nc-Spain1H

Eleven proteins related to carbohydrate metabolism were differentially abundant between isolates, with the greatest differences at 12 hpi. Ten proteins were more abundant in Nc-Spain1H: fructose-1,6-bisphosphatase (NCLIV_050070), fructose-1,6-bisphosphatase class 1 (NCLIV_050080), glycerol-3-phosphate dehydrogenase (NCLIV_001180), phosphoglucomutase (NCLIV_010960), phosphoenolpyruvate carboxykinase (NCLIV_041900), glucosamine:fructose-6-phosphate aminotransferase (NCLIV_031610), cytochrome c (NCLIV_060860) and orthologues of aspartate aminotransferase (NCLIV_064760), glycosyltransferase (NCLIV_004200) and citrate synthase I (NCLIV_037460), which showed a 2-2.7-fold higher abundance in Nc-Spain1H. During exponential growth (36 hpi), only the glucosamine-fructose-6-phosphate aminotransferase (NCLIV_031610) was 2-fold more abundant in Nc-Spain1H. At 56 hpi, there were no differences in these proteins between the isolates. Some of these proteins suggest that Nc-Spain1H fulfils a gluconeogenic function. Co-expression of enzymes involved in glycolysis and gluconeogenesis is a mechanism to rapidly adapt to changing nutrient conditions in their host cells [47] and could be an important glucose regulatory mechanism [48]. Over-expression of the function of gluconeogenesis in Nc-Spain1H may also indicate a failure in glucose salvage from the host cell and thus could be an important limiting factor for parasite growth. In relation to this hypothesis, the orthologue of the transporter/permease protein related to carbohydrate transport (NCLIV_039290) was more abundant in the highly virulent isolate Nc-Spain7 (3.3-fold). This carbohydrate transporter in Nc-Spain7 could facilitate the capture of glucose from the host and consequently the faster growth of this isolate.

Fatty acid biosynthesis in the apicoplast (FAS II system) and the metabolism of phospholipids are differentially regulated between isolates.

The apicoplast is indispensable for parasite survival and is the location of several anabolic pathways such as type II fatty acid [49]. Interestingly, orthologues of apicoplast triose phosphate translocator APT1 (NCLIV_026210) and beta-hydroxyacyl-acyl carrier protein dehydratase FABZ (NCLIV_004340), showed 2.8 and 2.4-fold higher abundance, respectively, in Nc-Spain7 at 12 hpi. The APT1 was again more abundant in Nc-Spain7 (2.3-fold) at 56 hpi. In *T. gondii,* APT1 is required for fatty acid synthesis in the apicoplast, but it also supplies the apicoplast with carbon skeletons for additional pathways and indirectly with ATP and redox equivalents [50]. In addition, APT1 has been shown to be an essential protein for parasite survival in *Toxoplasma* and *Plasmodium.*

Conversely, it is striking that the low virulence isolate Nc-Spain1H exhibited up-regulated recycling of the phospholipids pathway, (LAMP, http://www.llamp.net) at 36 and 56 hpi. Lipin protein (NCLIV_031190) and the glycerol-3-phosphate acyltransferase (NCLIV_029980) had 2.3 and 2.2-fold higher abundances, respectively, in Nc-Spain1H at 36 hpi. At 56 hpi, the glycerol-3-phosphate acyltransferase (NCLIV_029980) and the acyl-CoA synthetase (NCLIV_054250) had a 2-fold increased abundance in Nc-Spain1H. Phospholipids are the major lipid components of biological membranes, but lipids also serve as signalling molecules, energy stores, post-translational modifiers, and pathogenesis factors. It might be interesting to assess whether this up-regulation of proteins in Nc-Spain1H may be a strategy to counteract the effect of the lack of an apicoplast contribution.

All these metabolic differences between isolates could, at least partially, explain their phenotypic variations in growth if, as in *T. gondii,* strain-specific growth rates and virulence are driven by altered metabolic capacities [51].

3.5 Other key biological systems are also differentially represented between isolates.

Antioxidant and stress response systems

In *N. caninum* the importance of the production of IFN-gamma-induced NO in macrophages as a mechanism for killing intracellular *N. caninum* has been demonstrated [52]. To counteract this oxidative stress, parasites are equipped with specific ROS-detoxifying mechanisms that are critical for parasite survival and the establishment of infection [53]. The superoxide dismutase SOD2 (NCLIV_058830) had a 2-fold higher abundance in Nc-Spain1H TZP at 12 hpi. SOD2 in *T. gondii* is dually targeted to both the apicoplast and the mitochondrion of *T. gondii*, two organelles that require protection from oxidative stress [54]. Other proteins with oxidoreductase activity, such as the pyridine nucleotide-disulphide oxidoreductase family protein (NCLIV_029160), also showed a higher abundance in Nc-Spain1H at 12 hpi.

By contrast, another well-known antioxidant enzyme, the peroxiredoxin-2E-1 (NCLIV_014020), was more abundant in Nc-Spain7 throughout the entire tachyzoite lytic cycle. Peroxiredoxins provide another defence mechanism against oxidative damage and, in addition, some peroxiredoxins have been proposed as important immunomodulators in parasites [55,56]. Additionally, the putative serine/threonine protein phosphatase 5 (NCLIV_066900) and the orthologue of the NAD/NADP octopine/nopaline dehydrogenase (NCLIV_042450) displayed higher abundance in Nc-Spain7 at 12 hpi (2-2.5-fold) and 56 hpi (2.7-fold), respectively.

These findings could suggest that different ROS-detoxifying mechanisms are used by the different *N. caninum* isolates, which may contribute to their differing resistances to the host immune response.

Heat shock proteins are other stress-inducible proteins that can have important roles in parasite survival, although their functions are still unknown. Stress conditions associated with bradyzoite development induce the expression of HSPs such as HSP70

and HSP90 and HSP21 in *T. gondii* [57-59]. In the present work, the orthologue of HSP29 (NCLIV_041850), which is associated with the membrane of *T. gondii* [60], was 2-fold more abundant in Nc-Spain1H at 12 hpi.

Ubiquitin-proteasome system.

The ubiquitin-proteasome system plays a role the biological processes of parasites such as differentiation, cell cycle progression, proliferation and encystation [61]. The orthologue of serine carboxypeptidase s28 protein (NCLIV_008320) and peptidase, S9A/B/C family (NCLIV_063570), proteins related to the proteasome demonstrated a higher abundance at 36 (2.6 and 2.4-fold, respectively) and 56 (3.6 and 2.5-fold, respectively) hpi in Nc-Spain1H than in Nc-Spain7. Conversely, the ubiquitin family domain-containing protein (NCLIV_012950) and ubiquitin conjugation factor (NCLIV_019660), which are related to the ubiquitination process, were 2-fold more abundant in Nc-Spain7 at 56 hpi. In *T. gondii*, proteasome inhibitors do not affect host cell invasion but block parasite proliferation, daughter-cell budding, as well as DNA synthesis [61]. Furthermore, a study of the ubiquitin proteome of *T. gondii* has revealed a large number of ubiquitinated proteins localized to the cytoskeleton and inner membrane complex, as well as their roles as critical regulators of cell division and cell cycle transitions [62].

3.6 Nc-Spain1H and Nc-Spain7 tachyzoite transcriptome also showed marked variations between isolates but were inconsistent with the proteome results

We also investigated the transcriptome of Nc-Spain1H and Nc-Spain7 during early egress (56 hpi). Differential expression analysis revealed 550 DEGs between Nc-Spain1H and Nc-Spain7. Among these genes, 369 were over-expressed in Nc-Spain1H and 181 in Nc-Spain-7 (Supplemental file 5). The qPCR for RNA-Seq validation

displayed a profile similar to the RNA-Seq results, with a similar significance and direction of fold change in the nine genes analysed (Supplementary Fig. 3).

Furthermore, a comparison of the differentially expressed transcripts and the differentially expressed proteins at the same time-point showed that only 41 genes were differentially expressed at both levels. Among them, only approximately 50% of genes showed a consistent direction of fold change. When we compared DEGs and proteins with different abundances (FC>2), 6 matches were obtained. A few studies have reported a less than perfect correlation between transcript and protein expression, in Apicomplexan [63,64] and mammalian systems [65,66]. The reasons for this phenomena are multiple fold, including variations in protein degradation turn-over rates [67], differences in posttranslational regulation [68], cellular functions [69] and last but not the least, technical variations [70]. Despite the weak correlation found between the transcriptomic and proteomic data in this work, transcriptome and proteome profiles highlight some common distinctions among isolates.

Unfortunately, similarly to the proteomics results, a large portion (approximately 50%) of these DEGs are annotated as hypothetical proteins or proteins with unknown function, leading to a loss of interesting information. However, the transcriptome profiles showed differences in tachyzoite-bradyzoite conversion, secretory elements, metabolism and transcriptional regulation between isolates.

Bradyzoite-specific genes were highly expressed in the Nc-Spain1H isolate.

A remarkable result was the large number of bradyzoite-specific genes that were over-expressed in the low virulent isolate Nc-Spain1H (Table 1). The gene encoding the bradyzoite cytoplasmic antigen BAG1 (NCLIV_027470), which facilitates the transition from the tachyzoite to bradyzoite in *T. gondii* [71] had the largest fold change between isolates, demonstrating 140.6-fold higher expression in Nc-Spain1H. Other over-

expressed genes were the bradyzoite-specific surface antigens in *N. caninum* BSR4 (NCLIV_010030) and SAG4 (NCLIV_019580) [29,72]. Interestingly, as we have previous commented, SAG4 protein was also more abundant in the Nc-Spain1H isolate across the lytic cycle in this study. In addition to these stage-specific genes, the gene related to early tachyzoite conversion into bradyzoites, PMA1 (NCLIV_022240) [73] also displayed higher expression levels in the Nc-Spain1H isolate (23.6-fold). In addition, some isoenzymes involved in glycolysis (lactate dehydrogenase, enolase, glucose 6-phosphate isomerase) that are stage-specifically expressed in *T. gondii* and *N. caninum* bradyzoites [59,74] such as LDH2 (NCLIV_042910) and ENO1 (NCLIV_037490) were expressed at higher levels in Nc-Spain1H. The *N. caninum* gene orthologue of *T. gondii* deoxyribose phosphate aldolase-like, which is involved in the utilization of deoxyribose as a carbon and energy source in the bradyzoite stage [75], also exhibited higher expression in the Nc-Spain1H isolate. Genes related to the tissue cyst wall, such as NcMCP4 (NCLIV_003250) [76] and CST1 (NCLIV_040495), which play essential roles in the structural integrity and persistence of brain cysts [77], had 12-fold and 40.3-fold higher expression levels in the Nc-Spain1H isolate, respectively. Furthermore, higher expression levels of ribosomal proteins have been associated with strains that readily switch from the tachyzoite to bradyzoite in *T. gondii* [78]. This phenotype was also observed in the low virulence Nc-Spain1H isolate since 23 ribosomal proteins showed higher expression. It has been shown that Nc-Spain1H can start tachyzoite-bradyzoite conversion *in vitro* under induction conditions, although it is not really completed to encysted bradyzoites [32]. The bradyzoite-transcriptome and proteome profile expressed by the Nc-Spain1H isolate could be related to its slower growth rate. Interestingly, *T. gondii*, bradyzoite formation is preceded by, and critically dependent on, a parasite cell cycle shift towards slower growth [31]. These early

switching parasites have transcriptomes that are very similar to those of tachyzoites, indicating that these early developing parasites are largely slow-growing tachyzoites that can be considered pre-bradyzoites [79]. This pre-bradyzoite stage in Nc-Spain1H may explain, at least partially, its lower virulence in terms of causing abortion in cattle since tachyzoite growth (lower in strains that tend to form bradyzoites) is a phenotypic trait related to virulence in *N. caninum* and *T. gondii* [9,44,80].

Host cell attachment and invasion machinery is also differentially expressed between isolates.

Seventeen genes encoding for SRS displayed higher abundances in the Nc-Spain1H isolate, while only four were over-expressed in Nc-Spain7. These proteins are highly immunogenic, and their expression is thought to regulate the virulence of infection [26]. In the proteome analyses, only five proteins demonstrated different abundances between isolates, and the only one that matched between the transcriptome and proteome was the bradyzoite antigen SAG4.

In contrast to the proteome results, the transcriptome analyses revealed fewer microneme genes than SRS genes with differential expression between isolates. Seven had higher expression in Nc-Spain1H and only 2 in Nc-Spain7. According to the proteome results, MIC17B (NCLIV_038110) had higher expression in the Nc-Spain1H isolate. However, the gene encoding the TLN4 protein, with an increased abundance in the Nc-Spain7 proteome at 56 hpi, was expressed at a higher level in the Nc-Spain1H isolate.

Secretory effectors, rhoptry and dense granule proteins, also demonstrated differential mRNA expression between isolates.

Similarly to the proteomic results, the non-syntenic orthologue of *T. gondii* ROP24 was more highly expressed in the highly virulent isolate Nc-Spain7, and the non-syntenic

orthologue of *T. gondii* ROP1 (NCLIV_069110) was more highly expressed in the low virulent isolate Nc-Spain1H, but at 56 hpi instead of 12 hpi in the proteome. Another rhoptry protein with elevated expression in Nc-Spain1H was the predicted lineage-specific rhoptry kinase, subfamily ROPK-Eten1 (NCLIV_017420), which is present in the *T. gondii* ROP38/29/19 gene locus that has been found to be necessary to establish chronic infection in mice [81]. The only dense granule protein with differential expression (2-fold higher in Nc-Spain7) was GRA17 (NCLIV_005560), which in *T. gondii* leads to more rapid growth [82]. In the proteome studies, fewer differences were also found in these proteins, and no GRA proteins were differentially expressed at 56 hpi.

In *T. gondii*, two different sub-transcriptomes have been described, depending on the tachyzoite cell cycle phase. The G1-subtranscriptome characterized by the expression of genes related to biosynthetic and metabolic functions and the S/M-subtranscriptome enriched in specific genes for specialized apicomplexan processes, in which are included SAG, MIC and ROP proteins [83]. Because the observed differences in proteome elements and DNA transcription could be a consequence of a different progression across the tachyzoite cell cycle, we examined the DNA content in asynchronously growing Nc-Spain1H and Nc-Spain7 at 12, 36 and 56 hpi. At all time-points analysed, the flow cytometry results for the tachyzoites profiles showed that most parasites were in G1 and there were no differences between isolates (Fig. 5B), supporting a similar tachyzoite cell cycle status at the studied time-points.

Although these results showing elevated expression of host cell attachment and invasion machinery and secretory effectors related to virulence in the isolate with a reduced invasion rate and virulence are quite surprising, a recent study has shown that the genes

encoding these functions also exhibited elevated expressions in the Nc-Spain1H isolate at 12 hpi [16].

Different ApiAP2 repertoire may lead to differences in RNA expression and proteomes. Although the mechanisms underlying gene-specific regulation in Apicomplexan parasites are not completely known, the AP2 transcription factors in *T. gondii* have been associated with important functions including stage-specific gene activation, determination of differences between strains, parasite virulence and host invasion [78,79,84,85]. Most of the identified ApiAP2s in *N. caninum* (54 out of 68) are expressed during the tachyzoite stage, similar to *T. gondii* [27]. In our study, seven AP2 factors displayed higher expression in the highly virulence isolate Nc-Spain7 (AP2VIII-3, AP2VIII-4, AP2IX-8, AP2X-2, AP2X-11, AP2XI-1 and AP2XII-8) and two in the low virulence isolate Nc-Spain1H (AP2III-1 and AP2X-10). In the proteome, by contrast, no AP2 factors exhibited a differential abundance between isolates, which was likely due to lower sensitivity of the technique in comparison to RNA-Seq. Some of these factors have been found to be functional in stage-specific or cell cycle-regulated or even strain-specific expression in *T. gondii* [79], and thus a similar characterization in *N. caninum* would be very useful to better understand the regulation of gene expression in this parasite.

4. Concluding remarks

In this study, we performed proteome and transcriptome comparisons between two well-characterized *N. caninum* isolates and established marked differences and revealed the mechanisms potentially associated with phenotypic traits and virulence displayed by these isolates. The invasion machinery, metabolism, response to stress and the tendency to form bradyzoites have emerged as principal key factors for isolate behaviour and likely pathogenesis. However, it should be noted that the majority of DEGs and proteins

between isolates were annotated as hypothetical and proteins with unknown function. Enhancing the knowledge of this issue could be the best approach to unravel the mechanisms underlying the molecular basis of the virulence of *N. caninum*.

Furthermore, the weak correlation between gene expression and protein abundance highlighted the importance of post-transcriptional regulation in these parasites. High-throughput proteomics techniques such as LC-MS/MS therefore offer a more detailed picture than the transcriptome of mechanisms involved in phenotypic diversity and virulence in *N. caninum*. However, proteome analyses are also limited by additional post-transduction mechanisms involved in protein regulation (activation and protein turn over). Nevertheless, despite the weak correlation between the transcript and protein at the individual gene level, both datasets have identified, on a gene family level, a pre-bradyzoite status of the Nc-Spain1H isolate. This observation is very interesting since it could, at least partially, explain the reduced virulence of this isolate.

Altogether, the current study provides a global vision of the transcriptional and translational differences between isolates that display marked virulence differences, shedding light on a subset of proteins that are potentially involved in the pathogenesis of this parasite. New studies with a battery of well-characterized isolates may reveal common mechanism of *N. caninum* virulence. Our results lay the foundations for further investigations characterizing the relevance of such proteins in *N. caninum* pathogenesis and virulence.

Conflict of interest statement

The authors have declared no conflict of interest.

Acknowledgements

This work was supported by the Spanish Ministry of Economy and Competitiveness (AGL2013-44694-R), the Community of Madrid (PLATESA S2013/ABI2906) and the BBSRC (BB/L002477/1). The funders had no role in study design, data collection and analysis, decision to publish, or preparation of the manuscript. We acknowledge Dr. David Sibley from the Washington University School of Medicine (St. Louis, MO, USA) for the NcMIC2 antibody, Dr. Andrew Hemphill from the Institute of Parasitology, Vetsuisse Faculty (University of Bern, Switzerland) for the NcSAG1antibody and Dra. Aida Pitarch for advice in this work.

Author contributions

LMOM, JW, JRC, PH and ECF conceived and designed the experiments. JRC and PH carried out the tachyzoite samples collection for analyses. DX and NR performed RNA-Seq and LC/MS-MS analyses. PH performed the validation assays. DX performed bioinformatics analyses. PH, JRC and DX analysed data and wrote the manuscript. LMOM and NR critically revised the manuscript.

References

[1] J. Dubey, G. Schares, Neosporosis in animals—the last five years, Vet. Parasitol. 180 (2011) 90-108.

[2] M. P. Reichel, M. Alejandra Ayanegui-Alcérreca, L. F. P. Gondim, J. T. Ellis, What is the global economic impact of *Neospora caninum* in cattle – The billion dollar question, Int. J. Parasitol. 43 (2013) 133-42.

[3] A. L. Chryssafidis, G. Canton, F. Chianini, E. A. Innes, E. H. Madureira, S. M. Gennari, Pathogenicity of Nc-Bahia and Nc-1 strains of *Neospora caninum* in experimentally infected cows and buffaloes in early pregnancy, Parasitol. Res. 113 (2014) 1521-8.

[4] S. Rojo-Montejo, E. Collantes-Fernández, J. Blanco-Murcia, A. Rodríguez-Bertos, V. Risco-Castillo, L. M. Ortega-Mora, Experimental infection with a low virulence isolate of *Neospora caninum* at 70 days gestation in cattle did not result in foetopathy, Vet. Res. 40 (2009) 49.

[5] S. G. Caspe, D. P. Moore, M. R. Leunda, D. B. Cano, L. Lischinsky, J. Regidor-Cerrillo, G. Álvarez-García, I. G. Echaide, D. Bacigalupe, L. M. Ortega-Mora, A. C. Odeon, C. M. Campero, The *Neospora caninum*-Spain 7 isolate induces placental damage, fetal death and abortion in cattle when inoculated in early gestation, Vet. Parasitol. 189 (2012) 171-81.

[6] J. Regidor-Cerrillo, D. Arranz-Solís, J. Benavides, M. Gómez-Bautista, J. A. Castro-Hermida, M. Mezo, V. Pérez, L. M. Ortega-Mora, M. González-Warleta, *Neospora caninum* infection during early pregnancy in cattle: how the isolate influences infection dynamics, clinical outcome and peripheral and local immune responses, Vet. Res. 45 (2014) 10,9716-45-10.

[7] A. Hemphill, B. Gottstein, H. Kaufmann, Adhesion and invasion of bovine endothelial cells by *Neospora caninum*, Parasitology 112 (Pt 2) (1996) 183-97.

[8] A. Hemphill, N. Vonlaufen, A. Naguleswaran, N. Keller, M. Riesen, N. Guetg, S. Srinivasan, F. Alaeddine, Tissue culture and explant approaches to studying and visualizing *Neospora caninum* and its interactions with the host cell, Microscopy and Microanalysis 10 (2004) 602-20.

[9] J. Regidor-Cerrillo, M. Gómez-Bautista, I. Sodupe, G. Aduriz, G. Álvarez-García, I. Del Pozo, L. M. Ortega-Mora, In vitro invasion efficiency and intracellular proliferation rate comprise virulence-related phenotypic traits of *Neospora caninum*, Vet. Res. 42 (2011) 41.

[10] A. Dellarupe, J. Regidor-Cerrillo, E. Jiménez-Ruiz, G. Schares, J. M. Unzaga, M. C. Venturini, L. M. Ortega-Mora, Comparison of host cell invasion and proliferation among *Neospora caninum* isolates obtained from oocysts and from clinical cases of naturally infected dogs, Exp. Parasitol. 145 (2014) 22-8.

[11] L. Jiménez-Pelayo, M. García-Sánchez, J. Regidor-Cerrillo, P. Horcajo, E. Collantes-Fernández, M. Gómez-Bautista, N. Hambruch, C. Pfarrer, L. M. Ortega-Mora, Differential susceptibility of bovine caruncular and trophoblast cell lines to infection with high and low virulence isolates of *Neospora caninum*, Parasit. Vectors 10 (2017) 463.

[12] H. Beck, D. Blake, M. Dardé, I. Felger, S. Pedraza-Díaz, J. Regidor-Cerrillo, M. Gómez-Bautista, L. M. Ortega-Mora, L. Putignani, B. Shiels, A. Tait, W. Weir, Molecular approaches to diversity of populations of apicomplexan parasites, Int. J. Parasitol. 39 (2009) 175-89.

[13] E. G. Lee, J. H. Kim, Y. S. Shin, G. W. Shin, Y. R. Kim, K. J. Palaksha, D. Y. Kim, I. Yamane, Y. H. Kim, G. S. Kim, M. D. Suh, T. S. Jung, Application of proteomics for comparison of proteome of *Neospora caninum* and *Toxoplasma gondii* tachyzoites, J. Chromatogr. B. Analyt. Technol. Biomed. Life Sci. 815 (2005) 305-14.

[14] Y. S. Shin, G. W. Shin, Y. R. Kim, E. Y. Lee, H. H. Yang, K. J. Palaksha, H. J. Youn, J. H. Kim, D. Y. Kim, A. E. Marsh, J. Lakritz, T. S. Jung, Comparison of proteome and antigenic proteome between two *Neospora caninum* isolates, Vet Parasitol 134 (2005) 41-52.

[15] J. Regidor-Cerrillo, G. Álvarez-García, I. Pastor-Fernández, V. Marugán-Hernández, M. Gómez-Bautista, L. M. Ortega-Mora, Proteome expression changes among virulent and attenuated *Neospora caninum* isolates, J. Proteomics 75 (2012) 2306-18.

[16] P. Horcajo, L. Jiménez-Pelayo, M. García-Sánchez, J. Regidor-Cerrillo, E. Collantes-Fernández, D. Rozas, N. Hambruch, C. Pfarrer, L. M. Ortega-Mora, Transcriptome modulation of bovine trophoblast cells in vitro by *Neospora caninum*, Int. J. Parasitol. 47 (2017) 791-9.

[17] J. Regidor-Cerrillo, M. Gómez-Bautista, J. Pereira-Bueno, G. Adúriz, V. Navarro-Lozano, V. Risco-Castillo, A. Fernández-García, S. Pedraza-Díaz, L. M. Ortega-Mora, Isolation and genetic characterization of *Neospora caninum* from asymptomatic calves in Spain, Parasitology 135 (2008) 1651-9.

[18] J. A. Vizcaíno, A. Csordas, N. del-Toro, J. A. Dianes, J. Griss, I. Lavidas, G. Mayer, Y. Perez-Riverol, F. Reisinger, T. Ternent, Q. W. Xu, R. Wang, H. Hermjakob, 2016 update of the PRIDE database and its related tools, Nucleic Acids Res. 44 (2016) 447-56.

[19] B. Gajria, A. Bahl, J. Brestelli, J. Dommer, S. Fischer, X. Gao, M. Heiges, J. Iodice, J. C. Kissinger, A. J. Mackey, D. F. Pinney, D. S. Roos, C. J. Stoeckert Jr, H. Wang, B. P. Brunk, ToxoDB: an integrated *Toxoplasma gondii* database resource, Nucleic Acids Res. 36 (2008) 553-56.

[20] D. Xia, S. J. Sanderson, A. R. Jones, J. H. Prieto, J. R. Yates, E. Bromley, F. M. Tomley, K. Lal, R. E. Sinden, B. P. Brunk, D. S. Roos, J. M. Wastling, The proteome of *Toxoplasma gondii*: integration with the genome provides novel insights into gene expression and annotation, Genome Biol. 9 (2008) R116.

[21] L. Sheiner, J. L. Demerly, N. Poulsen, W. L. Beatty, O. Lucas, M. S. Behnke, M. W. White, B. Striepen, A systematic screen to discover and analyze apicoplast proteins identifies a conserved and essential protein import factor, PLoS Pathog. 7 (2011) e1002392.

[22] L. Pollo-Oliveira, H. Post, M. L. Acencio, N. Lemke, H. van den Toorn, V. Tragante, A. J. Heck, A. F. Altelaar, A. P. Yatsuda, Unravelling the *Neospora caninum* secretome through the secreted fraction (ESA) and quantification of the discharged tachyzoite using high-resolution mass spectrometry-based proteomics, Parasit. Vectors 6 (2013) 335.

[23] I. Pastor-Fernández, J. Regidor-Cerrillo, G. Álvarez-Garcia, V. Marugán-Hernández, P. García-Lunar, A. Hemphill, L. M. Ortega-Mora, The tandemly repeated NTPase (NTPDase) from *Neospora caninum* is a canonical dense granule protein whose RNA expression, protein secretion and phosphorylation coincides with the tachyzoite egress, Parasit. Vectors 9 (2016) 352.

[24] I. Pastor-Fernández, J. Regidor-Cerrillo, E. Jiménez-Ruiz, G. Álvarez-García, V. Marugán-Hernández, A. Hemphill, L. M. Ortega-Mora, Characterization of the

Neospora caninum NcROP40 and NcROP2Fam-1 rhoptry proteins during the tachyzoite lytic cycle, Parasitology 143 (2016) 97-113.

[25] UniProt Consortium, Activities at the Universal Protein Resource (UniProt), Nucleic Acids Res. 42 (2014) 191-98.

[26] C. Lekutis, D. J. Ferguson, M. E. Grigg, M. Camps, J. C. Boothroyd, Surface antigens of *Toxoplasma gondii*: variations on a theme, Int. J. Parasitol. 31 (2001) 1285-92.

[27] A. J. Reid, S. J. Vermont, J. A. Cotton, D. Harris, G. A. Hill-Cawthorne, S. Konen-Waisman, S. M. Latham, T. Mourier, R. Norton, M. A. Quail, M. Sanders, D. Shanmugam, A. Sohal, J. D. Wasmuth, B. Brunk, M. E. Grigg, J. C. Howard, J. Parkinson, D. S. Roos, A. J. Trees, M. Berriman, A. Pain, J. M. Wastling, Comparative genomics of the apicomplexan parasites *Toxoplasma gondii* and *Neospora caninum*: Coccidia differing in host range and transmission strategy, PLoS Pathog. 8 (2012) e1002567.

[28] Y. Adomako-Ankomah, G. M. Wier, A. L. Borges, H. E. Wand, J. P. Boyle, Differential locus expansion distinguishes Toxoplasmatinae species and closely related strains of *Toxoplasma gondii*, MBio 5 (2014) e01003-13.

[29] A. Fernández-García, V. Risco-Castillo, A. Zaballos, G. Álvarez-García, L. M. Ortega-Mora, Identification and molecular cloning of the *Neospora caninum* SAG4 gene specifically expressed at bradyzoite stage, Mol. Biochem. Parasitol. 146 (2006) 89-97.

[30] J. D. Wasmuth, V. Pszenny, S. Haile, E. M. Jansen, A. T. Gast, A. Sher, J. P. Boyle, M. J. Boulanger, J. Parkinson, M. E. Grigg, Integrated bioinformatic and targeted deletion analyses of the SRS gene superfamily identify SRS29C as a negative regulator of *Toxoplasma* virulence, MBio 3 (2012) e00321-12.

[31] M. E. Jerome, J. R. Radke, W. Bohne, D. S. Roos, M. W. White, *Toxoplasma gondii* bradyzoites form spontaneously during sporozoite-initiated development, Infect. Immun. 66 (1998) 4838-44.

[32] S. Rojo-Montejo, E. Collantes-Fernández, J. Regidor-Cerrillo, G. Álvarez-García, V. Marugán-Hernández, S. Pedraza-Díaz, J. Blanco-Murcia, A. Prenafeta, L. M. Ortega-Mora, Isolation and characterization of a bovine isolate of *Neospora caninum* with low virulence, Vet. Parasitol. 159 (2009) 7-16.

[33] F. M. Tomley, D. S. Soldati, Mix and match modules: structure and function of microneme proteins in apicomplexan parasites, Trends Parasitol. 17 (2001) 81-8.

[34] A. Naguleswaran, A. Cannas, N. Keller, N. Vonlaufen, G. Schares, F. J. Conraths, C. Bjorkman, A. Hemphill, *Neospora caninum* microneme protein NcMIC3: secretion, subcellular localization, and functional involvement in host cell interaction, Infect. Immun. 69 (2001) 6483-94.

[35] N. Keller, A. Naguleswaran, A. Cannas, N. Vonlaufen, M. Bienz, C. Bjorkman, W. Bohne, A. Hemphill, Identification of a *Neospora caninum* microneme protein (NcMIC1) which interacts with sulfated host cell surface glycosaminoglycans, Infect. Immun. 70 (2002) 3187-98.

[36] N. Keller, M. Riesen, A. Naguleswaran, N. Vonlaufen, R. Stettler, A. Leepin, J. M. Wastling, A. Hemphill, Identification and characterization of a *Neospora caninum* microneme-associated protein (NcMIC4) that exhibits unique lactose-binding properties, Infect. Immun. 72 (2004) 4791-800.

[37] J. Wang, D. Tang, W. Li, J. Xu, Q. Liu, J. Liu, A new microneme protein of *Neospora caninum*, NcMIC8 is involved in host cell invasion, Exp. Parasitol. 175 (2017) 21-7.

[38] H. Zhang, M. K. Compaore, E. G. Lee, M. Liao, G. Zhang, C. Sugimoto, K. Fujisaki, Y. Nishikawa, X. Xuan, Apical membrane antigen 1 is a cross-reactive antigen between *Neospora caninum* and *Toxoplasma gondii*, and the anti-NcAMA1 antibody inhibits host cell invasion by both parasites, Mol. Biochem. Parasitol. 151 (2007) 205-12.

[39] V. Lagal, E. M. Binder, M. H. Huynh, B. F. Kafsack, P. K. Harris, R. Diez, D. Chen, R. N. Cole, V. B. Carruthers, K. Kim, *Toxoplasma gondii* protease TgSUB1 is required for cell surface processing of micronemal adhesive complexes and efficient adhesion of tachyzoites, Cell Microbiol. 12 (2010) 1792-808.

[40] F. Parussini, I. Coppens, P. P. Shah, S. L. Diamond, V. B. Carruthers, Cathepsin L occupies a vacuolar compartment and is a protein maturase within the endo/exocytic system of *Toxoplasma gondii*, Mol. Microbiol. 76 (2010) 1340-57.

[41] M. S. Roiko, V. B. Carruthers, Functional dissection of *Toxoplasma gondii* perforin-like protein 1 reveals a dual domain mode of membrane binding for cytolysis and parasite egress, J. Biol. Chem. 288 (2013) 8712-25.

[42] F. Almeida, A. Sardinha-Silva, T. A. da Silva, A. M. Pessoni, C. F. Pinzan, A. C. Alegre-Maller, N. T. Cecilio, N. S. Moretti, A. R. Damasio, W. R. Pedersoli, J. R. Mineo, R. N. Silva, M. C. Roque-Barreira, *Toxoplasma gondii* Chitinase induces macrophage activation, PLoS One 10 (2015) e0144507.

[43] M. A. Hakimi, P. Olias, L. D. Sibley, *Toxoplasma* effectors targeting host signaling and transcription, Clin. Microbiol. Rev. 30 (2017) 615-45.

[44] L. D. Sibley, W. Qiu, S. Fentress, S. J. Taylor, A. Khan, R. Hui, Forward genetics in *Toxoplasma gondii* reveals a family of rhoptry kinases that mediates pathogenesis, Eukaryot. Cell 8 (2009) 1085-93.

[45] P. N. Ossorio, J. D. Schwartzman, J. C. Boothroyd, A *Toxoplasma gondii* rhoptry protein associated with host cell penetration has unusual charge asymmetry, Mol. Biochem. Parasitol. 50 (1992) 1-15.

[46] K. R. Buchholz, P. W. Bowyer, J. C. Boothroyd, Bradyzoite pseudokinase 1 is crucial for efficient oral infectivity of the *Toxoplasma gondii* tissue cyst, Eukaryot. Cell 12 (2013) 399-410.

[47] M. Blume, R. Nitzsche, U. Sternberg, M. Gerlic, S. L. Masters, N. Gupta, M. J. McConville, A *Toxoplasma gondii* gluconeogenic enzyme contributes to robust central carbon metabolism and is essential for replication and virulence, Cell Host Microbe 18 (2015) 210-20.

[48] A. M. Guggisberg, A. R. Odom, Sweet talk: regulating glucose metabolism in *Toxoplasma*, Cell Host Microbe 18 (2015) 142-3.

[49] G. I. McFadden, E. Yeh, The apicoplast: now you see it, now you don't, Int. J. Parasitol. 47 (2017) 137-44.

[50] C. F. Brooks, H. Johnsen, G. G. van Dooren, M. Muthalagi, S. S. Lin, W. Bohne, K. Fischer, B. Striepen, The *toxoplasma* apicoplast phosphate translocator links cytosolic and apicoplast metabolism and is essential for parasite survival, Cell Host Microbe 7 (2010) 62-73.

[51] C. Song, M. A. Chiasson, N. Nursimulu, S. S. Hung, J. Wasmuth, M. E. Grigg, J. Parkinson, Metabolic reconstruction identifies strain-specific regulation of virulence in *Toxoplasma gondii*, Mol. Syst. Biol. 9 (2013) 708.

[52] T. Tanaka, H. Nagasawa, K. Fujisaki, N. Suzuki, T. Mikami, Growth-inhibitory effects of interferon-gamma on *Neospora caninum* in murine macrophages by a nitric oxide mechanism, Parasitol. Res. 86 (2000) 768-71.

[53] S. S. Bosch, T. Kronenberger, K. A. Meissner, F. M. Zimbres, D. Stegehake, N. M. Izui, I. Schettert, E. Liebau, C. Wrenger, Oxidative stress control by apicomplexan parasites, Biomed. Res. Int. 2015 (2015) 351289.

[54] P. Pino, B. J. Foth, L. Y. Kwok, L. Sheiner, R. Schepers, T. Soldati, D. Soldati-Favre, Dual targeting of antioxidant and metabolic enzymes to the mitochondrion and the apicoplast of *Toxoplasma gondii*, PLoS Pathog. 3 (2007) e115.

[55] M. W. Robinson, A. T. Hutchinson, J. P. Dalton, S. Donnelly, Peroxiredoxin: a central player in immune modulation, Parasite Immunol. 32 (2010) 305-13.

[56] R. M. Fereig, Y. Nishikawa, Peroxiredoxin 3 promotes IL-12 production from macrophages and partially protects mice against infection with *Toxoplasma gondii*, Parasitol. Int. 65 (2016) 741-8.

[57] L. M. Weiss, Y. F. Ma, P. M. Takvorian, H. B. Tanowitz, M. Wittner, Bradyzoite development in *Toxoplasma gondii* and the hsp70 stress response, Infect. Immun. 66 (1998) 3295-302.

[58] P. C. Echeverria, M. Matrajt, O. S. Harb, M. P. Zappia, M. A. Costas, D. S. Roos, J. F. Dubremetz, S. O. Angel, *Toxoplasma gondii* Hsp90 is a potential drug target

whose expression and subcellular localization are developmentally regulated, J. Mol. Biol. 350 (2005) 723-34.

[59] V. Marugán-Hernández, G. Álvarez-García, V. Risco-Castillo, J. Regidor-Cerrillo, L. M. Ortega-Mora, Identification of *Neospora caninum* proteins regulated during the differentiation process from tachyzoite to bradyzoite stage by DIGE, Proteomics 10 (2010) 1740-50.

[60] N. de Miguel, P. C. Echeverria, S. O. Angel, Differential subcellular localization of members of the *Toxoplasma gondii* small heat shock protein family, Eukaryot Cell 4 (2005) 1990-7.

[61] C. Muñoz, J. San Francisco, B. Gutiérrez, J. González, Role of the ubiquitin-proteasome systems in the biology and virulence of protozoan parasites, Biomed. Res. Int. 2015 (2015) 141526.

[62] N. C. Silmon de Monerri, R. R. Yakubu, A. L. Chen, P. J. Bradley, E. Nieves, L. M. Weiss, K. Kim, The Ubiquitin proteome of *Toxoplasma gondii* reveals roles for protein ubiquitination in cell-cycle transitions, Cell Host Microbe 18 (2015) 621-33.

[63] T. W. Kooij, C. J. Janse, A. P. Waters, *Plasmodium* post-genomics: better the bug you know? Nat. Rev. Microbiol. 4 (2006) 344-57.

[64] J. M. Wastling, D. Xia, A. Sohal, M. Chaussepied, A. Pain, G. Langsley, Proteomes and transcriptomes of the Apicomplexa--where's the message? Int. J. Parasitol. 39 (2009) 135-43.

[65] T. Maier, M. Guell, L. Serrano, Correlation of mRNA and protein in complex biological samples, FEBS Lett. 583 (2009) 3966-73.

[66] R. de Sousa Abreu, L. O. Penalva, E. M. Marcotte, C. Vogel, Global signatures of protein and mRNA expression levels, Mol. Biosyst. 5 (2009) 1512-26.

[67] B. Schwanhausser, D. Busse, N. Li, G. Dittmar, J. Schuchhardt, J. Wolf, W. Chen, M. Selbach, Global quantification of mammalian gene expression control, Nature 473 (2011) 337-42.

[68] A. Battle, Z. Khan, S. H. Wang, A. Mitrano, M. J. Ford, J. K. Pritchard, Y. Gilad, Genomic variation. Impact of regulatory variation from RNA to protein, Science 347 (2015) 664-7.

[69] M. Jovanovic, M. S. Rooney, P. Mertins, D. Przybylski, N. Chevrier, R. Satija, E. H. Rodriguez, A. P. Fields, S. Schwartz, R. Raychowdhury, M. R. Mumbach, T. Eisenhaure, M. Rabani, D. Gennert, D. Lu, T. Delorey, J. S. Weissman, S. A. Carr, N. Hacohen, A. Regev, Immunogenetics. Dynamic profiling of the protein life cycle in response to pathogens, Science 347 (2015) 1259038.

[70] J. J. Li, P. J. Bickel, M. D. Biggin, System wide analyses have underestimated protein abundances and the importance of transcription in mammals, PeerJ 2 (2014) e270.

[71] Y. W. Zhang, K. Kim, Y. F. Ma, M. Wittner, H. B. Tanowitz, L. M. Weiss, Disruption of the *Toxoplasma gondii* bradyzoite-specific gene BAG1 decreases in vivo cyst formation, Mol. Microbiol. 31 (1999) 691-701.

[72] V. Risco-Castillo, A. Fernández-García, A. Zaballos, A. Aguado-Martínez, A. Hemphill, A. Rodríguez-Bertos, G. Álvarez-García, L. M. Ortega-Mora, Molecular characterisation of BSR4, a novel bradyzoite-specific gene from *Neospora caninum*, Int. J. Parasitol. 37 (2007) 887-96.

[73] M. Holpert, U. Gross, W. Bohne, Disruption of the bradyzoite-specific P-type (H+)-ATPase PMA1 in *Toxoplasma gondii* leads to decreased bradyzoite differentiation after stress stimuli but does not interfere with mature tissue cyst formation, Mol. Biochem. Parasitol. 146 (2006) 129-33.

[74] S. Tomavo, The differential expression of multiple isoenzyme forms during stage conversion of *Toxoplasma gondii*: an adaptive developmental strategy, Int. J. Parasitol. 31 (2001) 1023-31.

[75] A. Ueno, G. Dautu, B. Munyaka, G. Carmen, Y. Kobayashi, M. Igarashi, *Toxoplasma gondii*: Identification and characterization of bradyzoite-specific deoxyribose phosphate aldolase-like gene (TgDPA), Exp. Parasitol. 121 (2009) 55-63.

[76] K. R. Buchholz, H. M. Fritz, X. Chen, B. Durbin-Johnson, D. M. Rocke, D. J. Ferguson, P. A. Conrad, J. C. Boothroyd, Identification of tissue cyst wall components by transcriptome analysis of in vivo and in vitro *Toxoplasma gondii* bradyzoites, Eukaryot. Cell 10 (2011) 1637-47.

[77] T. Tomita, D. J. Bzik, Y. F. Ma, B. A. Fox, L. M. Markillie, R. C. Taylor, K. Kim, L. M. Weiss, The *Toxoplasma gondii* cyst wall protein CST1 is critical for cyst wall integrity and promotes bradyzoite persistence, PLoS Pathog. 9 (2013) e1003823.

[78] M. M. Croken, Y. Ma, L. M. Markillie, R. C. Taylor, G. Orr, L. M. Weiss, K. Kim, Distinct strains of *Toxoplasma gondii* feature divergent transcriptomes regardless of developmental stage, PLoS One 9 (2014) e111297.

[79] D. P. Hong, J. B. Radke, M. W. White, Opposing transcriptional mechanisms regulate *Toxoplasma* development, mSphere 2 (2017) e00347-16.

[80] J. P. Saeij, J. P. Boyle, J. C. Boothroyd, Differences among the three major strains of *Toxoplasma gondii* and their specific interactions with the infected host, Trends Parasitol. 21 (2005) 476-81.

[81] B. A. Fox, L. M. Rommereim, R. B. Guevara, A. Falla, M. A. Hortua Triana, Y. Sun, D. J. Bzik, The *Toxoplasma gondii* rhoptry kinome is essential for chronic infection, MBio 7 (2016) e00193-16.

[82] D. A. Gold, A. D. Kaplan, A. Lis, G. C. Bett, E. E. Rosowski, K. M. Cirelli, A. Bougdour, S. M. Sidik, J. R. Beck, S. Lourido, P. F. Egea, P. J. Bradley, M. A. Hakimi, R. L. Rasmusson, J. P. Saeij, The *Toxoplasma* dense granule proteins GRA17 and

GRA23 mediate the movement of small molecules between the host and the parasitophorous vacuole, Cell Host Microbe 17 (2015) 642-52.

[83] M. S. Behnke, J. C. Wootton, M. M. Lehmann, J. B. Radke, O. Lucas, J. Nawas, L. D. Sibley, M. W. White, Coordinated progression through two subtranscriptomes underlies the tachyzoite cycle of *Toxoplasma gondii*, PLoS One 5 (2010) e12354.

[84] R. Walker, M. Gissot, M. M. Croken, L. Huot, D. Hot, K. Kim, S. Tomavo, The *Toxoplasma* nuclear factor TgAP2XI-4 controls bradyzoite gene expression and cyst formation, Mol. Microbiol. 87 (2013) 641-55.

[85] R. Walker, M. Gissot, L. Huot, T. D. Alayi, D. Hot, G. Marot, C. Schaeffer-Reiss, A. Van Dorsselaer, K. Kim, S. Tomavo, *Toxoplasma* transcription factor TgAP2XI-5 regulates the expression of genes involved in parasite virulence and host invasion, J. Biol. Chem. 288 (2013) 31127-38.

Figure legends

Figure 1. Experimental design of the proteome and transcriptome analyses. Samples for proteome and transcriptome analyses were assayed in triplicate. (A) Photomicrographs for each time-point of sample collection at 400x. Black arrows indicate parasitophorous vacuoles at 12, 36 and 56 hpi. Red arrows indicate an area of recent egress. (B) Experimental design for proteome analyses. Tachyzoites were collected at 12, 36 and 56 hpi and purified using PD-10 columns. Purified tachyzoites were digested and analysed on an Easy-Spray column fused to a silica nanoelectrospray emitter coupled to a Q-Exactive mass spectrometer. For proteome data analyses, Progenesis QI (version 2.0, Nonlinear Dynamics) and Mascot (version 2.3, Matrix Science) for peptide identification were used. (C) Experimental design for transcript analyses. Total RNA was isolated from purified tachyzoites, and then polyadenylated RNA was purified and used to prepare RNA-seq libraries. Libraries were sequenced with HiSeq2500. The TopHat2 aligner was used to align sequencing reads against the reference genome, and the Cufflinks software (version 2.1.1) was applied to assemble transcripts, quantify expression levels and analyse differentially expressed genes.

Figure 2: **Volcano plot showing the proteome results**. (A) Volcano plot of differentially abundant proteins at 12 hpi. (B) Volcano plot of differentially abundant proteins at 36 hpi. (C) Volcano plot of differentially abundant proteins at 56 hpi. The 'x' axis represents the log fold-change of different protein abundances (Nc-Spain1H vs Nc-Spain7), and 'y' axis represents the negative log of the p value. Proteins have been grouped and coloured in the main categories: host attachment and invasion in red, metabolic processes in green, other biological systems in purple and unannotated proteins in grey. The dotted line represents the position of the fold change = 2, from which the differences in abundance are considered significant.

Figure 3. Venn diagrams showing the number of differentially abundant proteins between Nc-Spain1H and Nc-Spain7 isolates across tachyzoite lytic cycle. (A) The total number of proteins increased in abundance (fold change ≥ 2) in the Nc-Spain1H isolate each time-point of the lytic cycle (12 hpi, 36 hpi and 56 hpi). (B) The total number of proteins increased in abundance (fold change ≥ 2) in the Nc-Spain7 isolate at 12 hpi, 36 hpi and 56 hpi. Proteins are listed in Supplemental file 4.

Figure 4. Number of proteins with higher abundance in each isolate grouped in functional categories. (A) Number of proteins with higher abundance in each isolate at 12 hpi, (B) number of proteins with higher abundance in each isolate at 36 hpi and (C) number of proteins with higher abundance in each isolate at 56 hpi.

Figure 5: Invasion rates and flow cytometry profiles of Nc-Spain1H and Nc-Spain7 tachyzoites. (A) Graphs represent parasite infection rates defined as the percentage of invaded tachyzoites. Bars represent median invasion rates, and each point represents invasion rates determined for 4 replicates from 3 independent assays. (**) indicates $P < 0.01$ (Mann-Whitney U-test). (B) Representative flow cytometric histograms showing the distribution of tachyzoites in each cell cycle phase using a propidium iodide stain.

The table shows the average percentages of G1 and G2/M tachyzoites. The green lines show the Nc-Spain7 isolate, and the black lines show the Nc-Spain1H isolate.

Table 1. Bradyzoite-related genes with higher expression in Nc-Spain1H isolate.

Gene ID[1]	Ortholog in *T. gondii*	Gene Product	Fold change[2]
NCLIV_027470	TGME49_259020	BAG1*	142.65
NCLIV_010030	TGME49_320230	BSR4	3.9
NCLIV_019580	TGME49_280570	SAG4	36.39
NCLIV_022240	TGME49_252640	PMA1*	23.6
NCLIV_042910	TGME49_291040	LDH2*	114.14
NCLIV_037490	TGME49_268860	ENO1*	23.22
NCLIV_010810	TGME49_318750	Deoxyribose-phosphate aldolase	42.61
NCLIV_003250	TGME49_208730	NcMCP4	11.97
NCLIV_040495	TGME49_264670	CST1*	40.29

[1]In addition to these genes, 23 ribosomal proteins had increased its expression in Nc-Sapin1H, a higher expression level of ribosomal proteins have been associated with strains that readily switch from tachyzoite to bradyzoite in *T. gondii* [78].

*Protein names are assigned from *T. gondii* orthologues because lack of *N. caninum* annotations

[2]Fold change of the expression levels in the Nc-Spain1H comparing to Nc-Spain7

Fig. 1

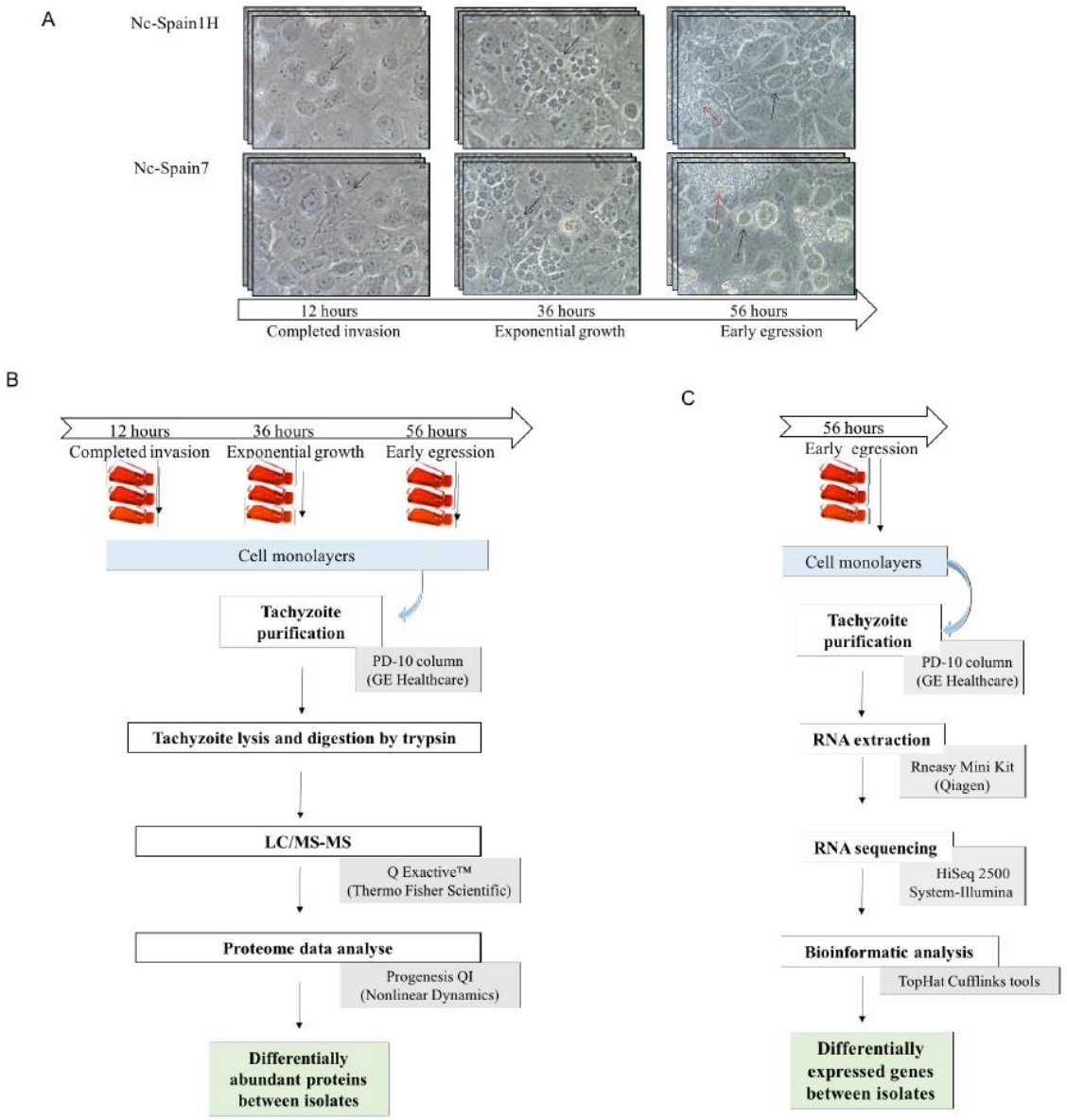

Fig. 2

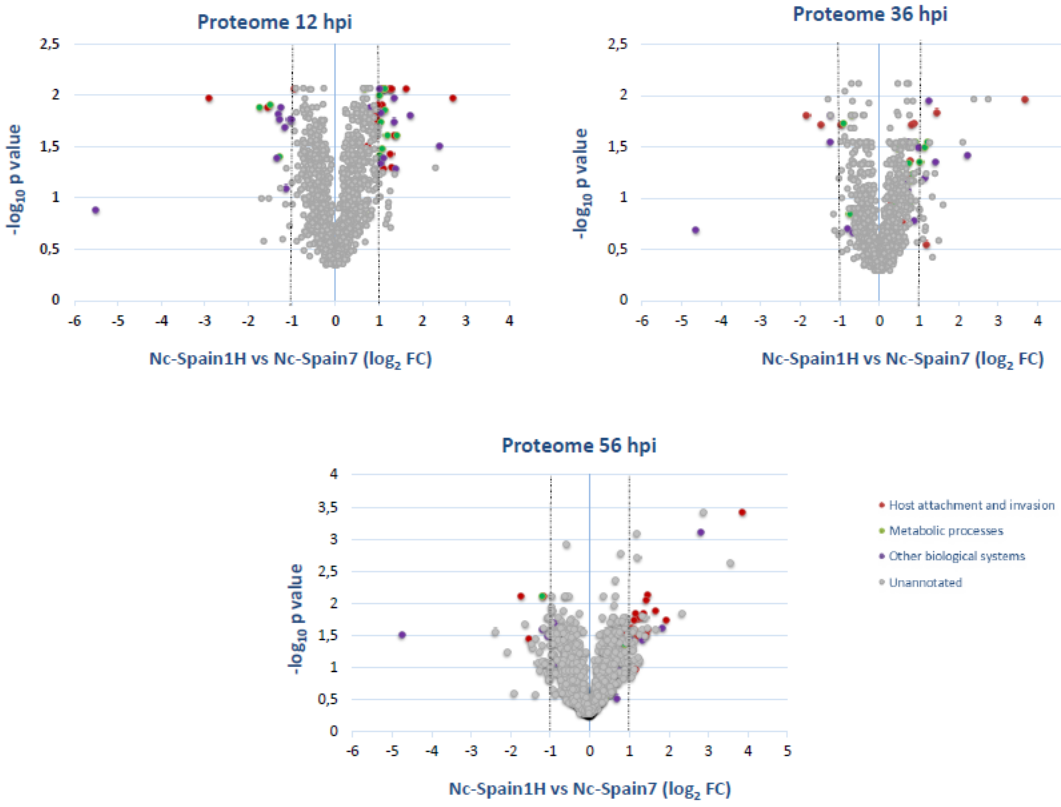

Fig. 3

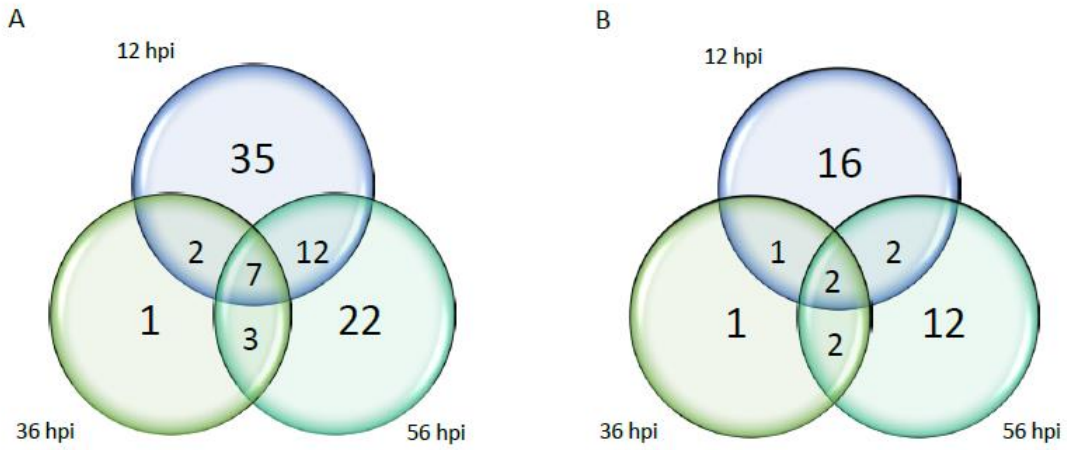

Fig. 4

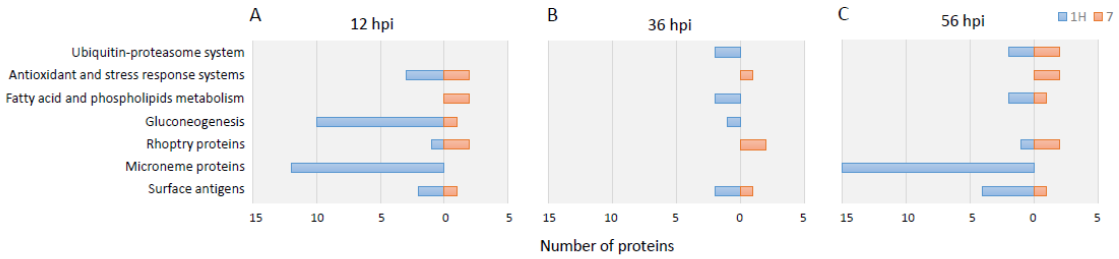

Fig. 5

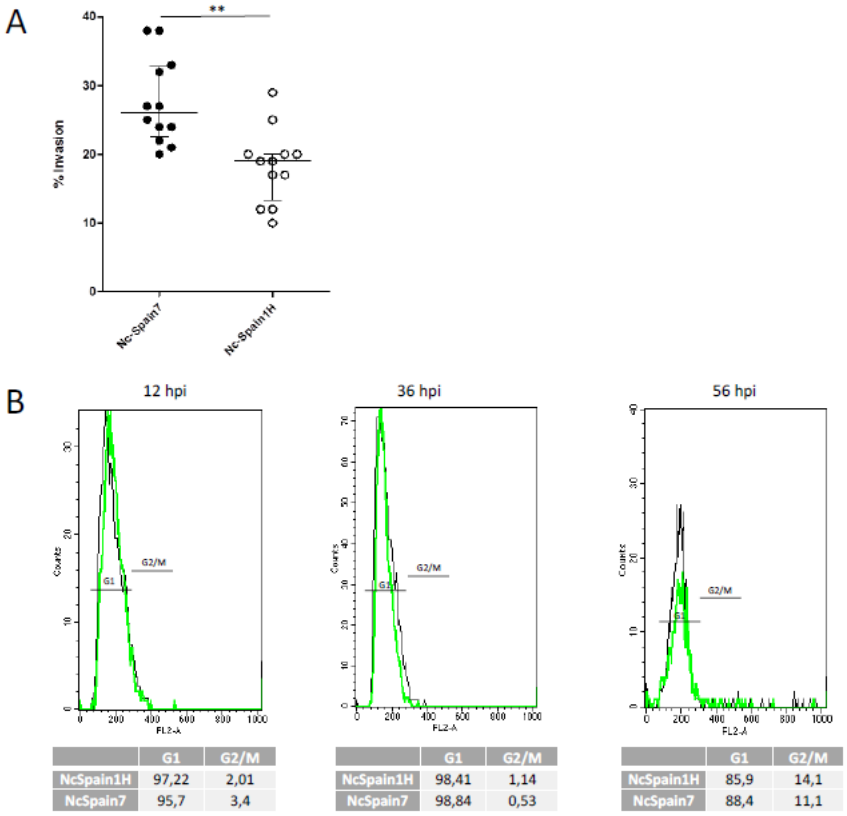

	G1	G2/M
NcSpain1H	97,22	2,01
NcSpain7	95,7	3,4

	G1	G2/M
NcSpain1H	98,41	1,14
NcSpain7	98,84	0,53

	G1	G2/M
NcSpain1H	85,9	14,1
NcSpain7	88,4	11,1

Graphical abstract

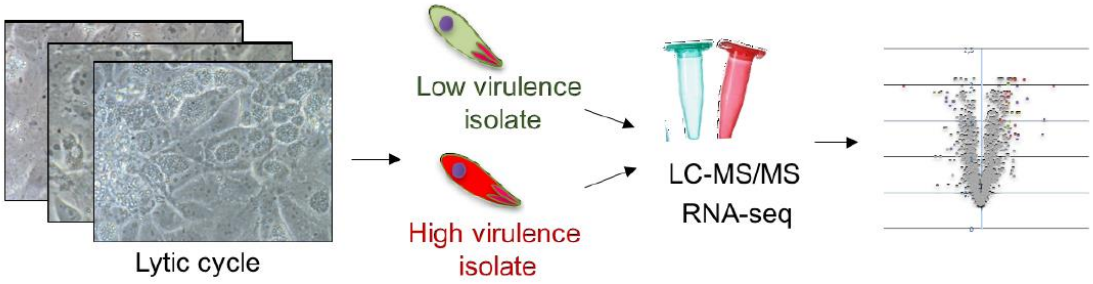

Highlights

- LC-MS/MS was used to characterize the proteomes of two *N. caninum* isolates throughout the lytic cycle
- High and low virulent isolates of *N. caninum* display different proteomes throughout the lytic cycle
- RNA-seq was used to characterize the transcriptome of *N. caninum* isolates in early egress
- Transcriptomes showed marked variations between isolates but were inconsistent with the proteome results
- Transcriptome and proteome of the low virulence isolate identified a pre-bradyzoite status of this isolate

Significance

The molecular basis that govern biological variability in *N. caninum* and the pathogenesis of neosporosis have not been well-established yet. This is the first study in which high throughput technology of LC-MS/MS and RNAseq is used to investigate differences in the proteome and transcriptome between two well-characterised isolates. Both isolates displayed different proteomes throughout the lytic cycle and the transcriptomes also showed marked variations but were inconsistent with the proteome results. However, both datasets identified a pre-bradyzoite status of the low virulence isolate Nc-Spain1H. This study reveals interesting insights into likely mechanisms involved in virulence in *N. caninum* and shed light on a subset of proteins that are potentially involved in the pathogenesis of this parasite